ELSEVIER

Journal of Photochemistry and Photobiology A: Chemistry 104 (1997) 179–187

Journal of PHOTOCHEMISTRY AND PHOTOBIOLOGY A:CHEMISTRY

Photophysics of a "simple" cyanide dye [1]

M.R.V. Sahyun [2], J.T. Blair

Information, Imaging and Electronics Sector Laboratories, 3M Center, St. Paul, MN 55144, USA

Received 18 March 1996; accepted 19 August 1996

Abstract

We have studied the photophysics of 1,1′-diethyl-2,2′-cyanine p-toluenesulphonate (I) by absorption and fluorescence spectroscopy. Quantum yields are reported for its fluorescence in a series of alcohol solvents, and analyzed according to the model of Vogel and Rettig. We detect two rapidly equilibrating forms of I in solution, each with unique fluorescence, designated the V- and W-bands, respectively. We identify these forms with *anti*- and *syn*-I. Quantum chemical and molecular mechanics calculations support this assignment. Observation of some V-band emission on excitation of the W-isomer implies dual fluorescence from *anti*-I. Time-resolved laser flash spectroscopy shows that recovery of the ground state of I lags the decay of both fluorescences, which occurs on the picosecond time scale. We assign this effect to repopulation of the ground state exclusively from a twisted intermediate funnel state which undergoes radiation-less deactivation only on the nanosecond time scale.

N,N-dimethylaniline (DMA) quenches both fluorescences of I with a Stern–Volmer concentration dependence. *N,N*-dimethyl-p-toluidine (DMT) quenches the V-band but enhances W-band emission. We analyze these results in terms of π-complexation of I by the quenchers. The W-form of I adsorbs to nanoparticulate AgBr which supports its assignment as the syn-isomer. Fluorescence quantum efficiency is enhanced on adsorption, but adsorbate fluorescence is quenched by both DMA and DMT. Quenching shows a Perrin equation concentration dependence. We assign it to long-range electron transfer between adsorbed quencher and excited dye, which, in turn, we relate to the mechanism of super-sensitization in silver halide photography. © 1997 Elsevier Science S.A.

Keywords: Photophysics; Cyanine dye

1. Introduction

The photophysics of cyanine dyes are of continuing interest owing to their utility as spectral sensitizers in photography [1], in biomedical applications [2], and in laser technology [3]. In solution their fluorescence quantum efficiency may be very low owing to facile radiationless decay. This process involves torsional motion about bonds in the polymethine chain of the dye, as demonstrated by fluorescence depolarization studies [4]. Fluorescence efficiencies are particularly low in the shortest chain members of the series where steric hindrance may preclude coplanarity of the aromatic nuclei, even in the ground state [3a,5]. Fluorescence efficiency can be greatly enhanced when the dye is adsorbed to a substrate [6,7] or incorporated into an organized assembly [2]. In such environments the torsional pathway for radiationless deactivation is thought to be inhibited.

Recently, using elegant femtosecond laser techniques Åberg et al. [8] have shown that this torsional relaxation process, leading to syn–anti isomerization, is barrierless for the case of the simple, but sterically hindered 1,1′-diethyl-4,4′-cyanine cation. The potential energy surface used by these authors to interpret their results suggested that it might be possible to observe dual fluorescence from such a dye. This expectation is supported by the report of stimulated emission from photoisomers of certain symmetrical dyes under conditions of laser pumping, leading to two-band lasing [9]. It should also be possible to effect substantial perturbation of the potential surface for isomerization through ground-state π-complexation of the chromophore. Observation of triplet exciplex formation between a cyanine dye and aromatic amines in dilute polyvinylchloride solid solution implies that such complexes exist in ground as well as excited states, although they are not detected by optical absorption spectroscopy [10].

The present study explores these possibilities for the case of 1,1′-diethyl-2,2′-thiacyanine p-toluenesulphonate (I), in solution and adsorbed on AgBr. These systems are probed by conventional steady-state absorption and emission spec-

[1] This paper is contribution no. 95-0264CX from the Information, Imaging and Electronics Sector Laboratories, 3M Center, St. Paul, MN 55144, USA.

[2] Present address: Department of Chemistry, University of Wisconsin, Eau Claire, WI 54702, USA.

PII S1010-6030(96)04481-4

troscopy and time-resolved emission spectroscopy. The study also attempts to assess the implications of these processes for spectral sensitization of the silver halide photography.

2. Experimental details

2.1. Materials

Dye I, prepared by ion exchange of the commercially available (H.W. Sands Corp.) iodide salt, was available in our laboratories in high purity from another study. Purity was verified by thin layer chromatography. Solvents were spectroscopic quality (EM Omnisolv^R methanol and ethanol, Aldrich spectro-photometric grade 1-propanol, and Aldrich "99+%" 1-pentanol). Amine quenchers were redistilled from the products of commerce over KOH and stored protected from light. The quenchers did not by themselves contribute to the fluorescence observable in the bandpass in which quenching of I was studied.

For experiments on silver bromide, a nanosol (1×10^{-4} M AgBr in ethanol) was prepared as previously described [11]. In that study we showed both by optical absorption spectroscopy and X-ray diffractometry the mean particle diameter of this material to be 60 Å. The colloid is indefinitely stable when prepared in a ca. 10% excess of halide. Under these conditions spheroidal particles with negatively charged, primarily {111} faces should be obtained. The advantages of such a nanosol over dispersions of photographic AgBr crystals [6] for the present study include a large surface area for adsorption of dye and absence of light scattering. The latter would interfere with the intended transmission spectroscopic measurements.

2.2. Methods

Absorption spectra were recorded on a Coleman–Hitachi EPS-3T dual beam spectrophotometer. Wavelength calibration was carried out immediately prior to the experiments. Fluorescence measurements were carried out on a Perkin–Elmer MPF-44b spectrophotometer modified to include a Mamamatsu R936 photomultiplier tube, lock-in amplification, and digital output. Raw data were corrected on a wavelength-by-wavelength basis by reference to a "look-up" table created by measuring instrument response to a white card for $\lambda_{em}=\lambda_{ex}$ over the spectral regime under investigation. As configured, the fluorimeter was sensitive to emission at quantum efficiency levels of $\geq5\times10^{-4}$, with wavelength resolution of ±4 nm. Fluorescence quantum yields were estimated by comparison of the emission intensity of I at 23 ± 5 °C, integrated over the fluorescence bandpass of the emission band under investigation, with that of Coumarin 343 (Eastman Kodak laser grade) in methanol, at a concentration yielding the same optical density as the test solution at the wavelength of excitation.

Fluorescence lifetime measurements were made on 2.5×10^{-5} M solutions of I in 2 mm quartz cuvettes excited by 30 ps (FWHM) pulses from an unamplified Nd:YAG laser, frequency tripled to 355 nm [12a]. Emission was monitored from the front of the sample by a Hamamatsu streak camera [12b]; data recording and analysis were carried out as previously described [12]. For laser flash photolysis monitored by transient absorption spectroscopy, the output of the same Nd:YAG laser was amplified in two stages to 1.0 ± 0.2 mJ per pulse at 355 nm. Under these conditions it was found that ca. 25% of the dye molecules in solution were excited in one pulse. At least eight complete spectra were recorded for each delay time as previously described [13], and computer averaged to yield the spectra from which kinetic data were extracted.

2.3. Computational studies

For reasons of cost and economy of computer usage the computational work was carried out primarily at the semi-empirical level using the PM3 semi-empirical parameter set [14] and supplemented with some ab initio computation to obtain improved accuracy. The main computational tool employed was SPARTAN [15], which allows both semi-empirical and ab initio computations on molecular systems. GAUSSIAN 94 [16], running on a Cray C90, was used for additional ab initio calculations. For calculation of excitation energies it was necessary to incorporate configuration interaction. Dye molecule excitations can be approximated as single electron events. Thus we considered it adequate to use configuration interaction with only single electron configurations (CIS).

For each isomer of I considered (*syn*-I and *anti*-I) a molecular mechanics geometry search was carried out to find the minimum energy starting point. From this point a full PM3 geometry optimization was carried out. The single point CIS computations were then performed at the minimum-energy PM3 geometry. After these semi-empirical calculations, an ab initio geometry optimization was carried out starting from the PM3 minimum. This computation was at the Hartree–Fock split valence level HF/3-21G [17]. At the ab initio minimized geometry, a final ab initio CIS computation was carried out to find excitation energies and oscillator strengths.

3. Results and discussion

3.1. Absorption and emission spectra

The absorption spectrum of I (2.5×10^{-6} M in methanol) is shown in Fig. 1: $\lambda_{max}=422.5$ nm, $\epsilon=1.2\times10^5\,M^{-1}\,cm^{-1}$ and $\Delta\nu_{1/2}=2250\,cm^{-1}$. We accordingly estimate the natural lifetime, τ_{nat}, for the Franck–Condon state as 2.0 ± 0.3 ns [18]. The emission spectrum was recorded with $\lambda_{ex}=420$ nm, close to λ_{max} of the absorption spectrum, as shown in Fig. 2(a). This spectrum is obviously not a mirror image of

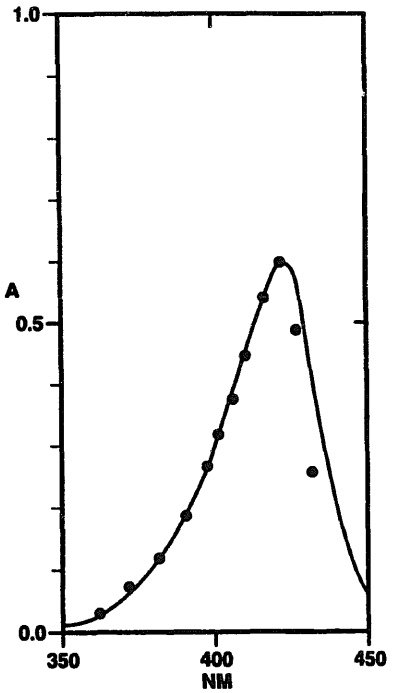

Fig. 1. Absorption spectrum of I in methanol (5×10^{-6} M); data points correspond to simulation of the spectrum by combination of the V- and W-band excitation spectra (see text).

the absorption spectrum, which was initially surprising. Upon further examination it became apparent that the emission spectrum could be deconvoluted into two components: on centered on 440 nm ($h\nu=2.85$ eV) and the other centered on 480 nm ($h\nu=2.60$ eV), as also shown in Fig. 2(a). These are designated the V- and W-bands, respectively. The excitation spectra recorded with $\lambda_{em}=480$ nm (W-band) strongly resembled the absorption spectrum with $\lambda_{max}=422$ nm, but the absorption envelope was somewhat narrower ($\Delta\nu_{1/2}=1450\ cm^{-1}$). This trace is also shown in Fig. 2(a); it appears to be a mirror image of the V-band emission spectrum.

When the excitation spectrum was recorded with $\lambda_{em}=440$ nm (V-band), a bimodal distribution of activity was found, as shown in Fig. 2(b), which strongly suggests deconvolution into two Gaussian bands. The maxima are located at 395 nm and 422 nm. The longer wavelength component corresponds to the excitation spectrum of Fig. 2(a). Excitation at 395 nm yielded an emission spectrum that more closely resembled a reflection of the absorption band, though again narrower, as also shown in Fig. 2(b).

We found that we could represent the absorption spectrum as a weighted sum of the W- and V-band excitation spectra, with the two distributions contributing 87% and 13%, respectively, as shown in Fig. 1. We hypothesize that in solution dye I exists as a dynamically equilibrating mixture of the syn- and anti-isomers, corresponding to the 422 nm and 395 nm absorptions, respectively. The major isomer is accordingly responsible for W-band emission, and the minor isomer is responsible for V-band emission. The existence and rapid equilibration of more than one ground-state conformation has

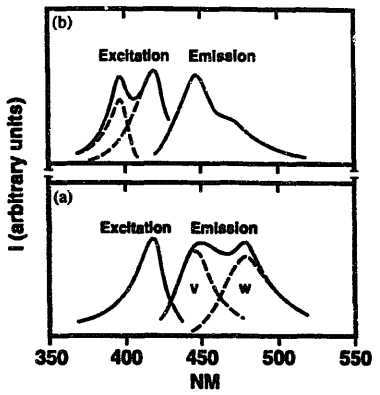

Fig. 2. Fluorescence emission and excitation spectra for I in methanol: (a) fluorescence spectrum excited at 420 nm and deconvoluted into V- and W-components (dashed lines); excitation spectrum corresponding to 480 nm emission; (b) fluorescence spectrum excited at 395 nm; excitation spectrum corresponding to 440 nm emission deconvoluted into two components (dashed lines).

also been inferred for a thiacarbocyanine dye [19]. If our assignment is correct, observation of some V-band emission on excitation into the W-isomer absorption (422 nm) band implies W-to-V isomerization along the excited-state potential surface, as expected from the model of Åberg et al. [8].

The fluorescence quantum yield, Φ_f, was estimated by comparison to the emission from Coumarin 343 at comparable optical density at λ_{ex}. These measurements were made in four primary alcohol solvents of differing viscosities to allow analysis according to the model of Vogel and Rettig [20]. Accordingly the rate constant for non-radiative decay, k_{nr}, comprises viscosity (η)-independent, k_o, and viscosity-dependent, k_η, components; the latter is associated with the processes coupling torsional motion about the central methine carbon atom in I.

$$k_{nr}=k_o+k_\eta(\eta^{-\alpha}) \quad (1)$$

where α is a measure of the relative contribution of Stokes diffusion of the rotating molecular fragment and diffusion of the dye molecule into free volume, where there is no frictional barrier to isomerization. Thus

$$\alpha=1-(E_2/E_\eta) \quad (2)$$

where E_2 is the activation energy for diffusion into free volume and E_η is the corresponding parameter for Stokes diffusion. Given that

$$\Phi_f=k_r/(k_r+k_{nr}) \quad (3)$$

where $k_r=1/\tau_{nat}$

$$\Phi_f^{-1}=1+(k_o/k_r)+(k_\eta/k_r)\eta^{-\alpha} \quad (4)$$

Fluorescence quantum yields and data for the analysis according to Eq. (4) are given in Table 1, including the correlation coefficients, r. In all cases, k_o was found to be within experimental error of zero. This result differs from that obtained by Schuster et al. [21] from the study of the effect of pressure on fluorescence of higher order carbocyanine dyes. Aramendia et al. [22] have associated k_o with internal conversion

Table 1
Fluorescence quantum yield data for I in various alcohol solvents; analysis according to Eq. (4)

Solvent	η(cP @20 °C)	Φ_f(V-band)	Φ_f(W-band)
Methanol	0.59	0.013	0.003
Ethanol	1.20	0.020	0.005
1-Propanol	2.25	0.027	0.0075
1-Pentanol	3.95	0.035	0.010
Analysis			
α		0.51	0.67
k_η/k_r		55	232
r		0.998	0.999
k_η		$(2.8\pm0.8)\times10^{10}$	$(1.6\pm0.5)\times10^{11}$ s^{-1}

processes involving energy acceptance by modes of the polymethine chain which is absent in I.

Absolute values of k_η are estimated in Table 1 using the approximate value of τ_{nat} above. It is apparent that torsional relaxation of the W-isomer is close to barrierless, while a small activation barrier must obtain for similar relaxation of the V-isomer. This feature was not included in the potential surface calculated, albeit for a different dye, by Åberg et al. [8]. Significantly, the non-radiative decay rates of neither the V- nor the W-species reflect solvent dielectric relaxation times [23] which, for linear alcohols, scale approximately with η^2.

3.2. Computational studies

In order to support our assignment above, that W- and V-I correspond to its syn- and anti-isomers, respectively, computations were carried out at the semi-empirical level with ab initio refinement. Results (dihedral angles between the planes of the benzthiazolyl nuclei, heats of formation, dipole moments, λ_{max}, and oscillator strengths) are given in Table 2. For all levels computed, the anti-isomer is unambiguously at a higher energy than its syn-counterpart, consistent with the assignment of V-band absorption and emission to the anti-isomer, and of W-band absorption and emission to the syn-form. Both semi-empirical and ab initio computations find the anti-isomer to be significantly twisted out of plane, with a dihedral angle of 31–32° between the benzthiazolyl nuclei. In the syn-form these nuclei are surprisingly co-planar. Ab initio optimized geometries are shown in a ball-and-stick representation in Fig. 3.

Table 2
Computational characterization of *syn*- and *anti*-I

Calculation type	*Syn*-I	*Anti*-I	Difference
SPARTAN with PM3 geometry optimization:			
Dihedral angle	0°	32°	
Heat of formation	229.8	236.2	6.4 kcal mol^{-1}
Dipole moment	2.75	0.93 D	
SPARTAN with CIS at PM3 optimized geometry:			
λ_{max}	469.8	488.1	18.3 nm
Oscillator strength	1.36	1.04	
GAUSSIAN 94 with HF/3-21G geometry optimization:			
Dihedral angle	0°	31°	
Total energy	−1625.7341	−1625.7143	0.0198 a.u. = 12.4 kcal mol^{-1}
GAUSSIAN 94 with CIS at ab initio optimized geometry:			
λ_{max}	272.4	281.2	8.8 nm
Oscillator	1.41	1.37	

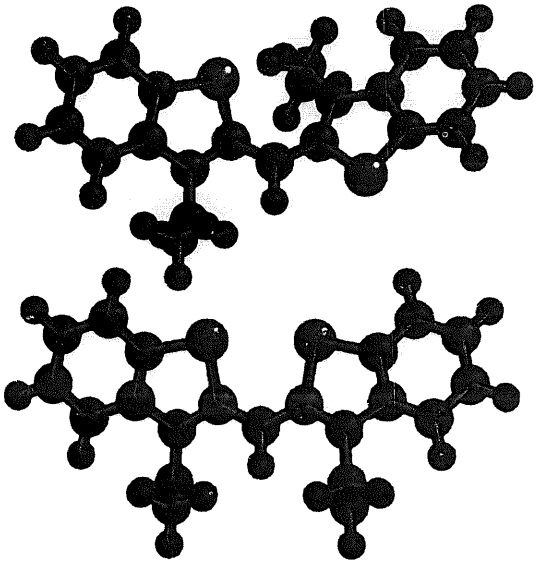

Fig. 3. Ball-and-stick representations of ab initio optimized geometries for *syn*-I (below) and *anti*-I (above).

The computed excitation energies (as λ_{max}) are not in agreement with experiment, though the semi-empirical result obtained with SPARTAN and geometry optimization at the PM3 level, incorporating CIS, provides more reasonable estimates of λ_{max}. At both computational levels excitation of *syn*-I is predicted to occur at slightly higher energy (shorter wavelength) than for *anti*-I. the opposite is the case in reality, if the assignments consistent with the relative total energies are correct.

3.3. Time-resolved experiments

Both methanol and pentanol solutions of I were excited at 355 nm using ca. 30 ps laser pulses. V- and W-band emissions were isolated using narrow bandpass filters. Neither rise nor fall of either emission were distinguishable from the laser pulse profile within experimental error. This result suggests that the radiative lifetimes of both species in both solvents are fast in comparison to the pulse width. From the data of Table 1 we expect the longest radiative lifetime (for V-band emission in 1-pentanol) to be no more than 70 ps, consistent with this inference. We did not observe any delayed fluorescence. However, the V-state, for example, may be populated very rapidly from the W-state; if torsional relaxation of W-I

were rate determining, then the V-conformation could be established within 20 ps.

When the flash excitations of I in either methanol or pentanol were monitored by time-resolved absorption spectroscopy, we observed both bleaching of the 422 nm absorption band and the appearance of a light absorbing transient centered on ca. 450 nm, which we assign to a relatively long-lived excited state. Representative spectra are shown in Fig. 4. Decay of the light absorbing transient and recovery of the ground state were analyzed as first-order processes. Kinetic plots for experiments in methanol and pentanol are shown in Fig. 5. It can be seen that recovery of the ground state and decay of the light absorbing transient occur in parallel, with characteristic lifetimes of 0.5 ± 0.1 ns in methanol and 1.0 ± 0.2 ns in pentanol. These time constants clearly are not identifiable with the measured fluorescence lifetimes but

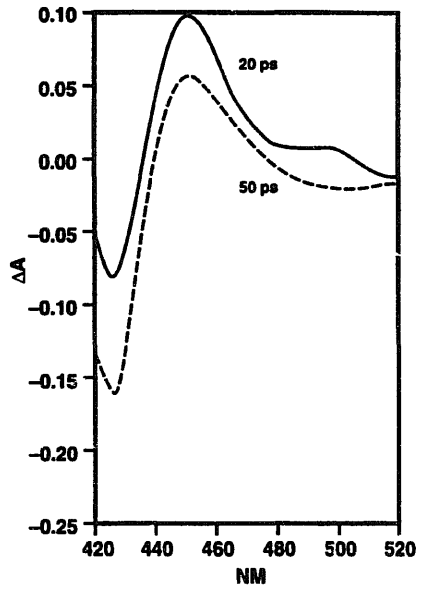

Fig. 4. Representative, smoothed transient absorption spectra showing bleaching of the principal absorption band of I (negative ΔA) at 422 nm and formation of the light absorbing transient (positive ΔA) at 450 nm, recorded 20 and 50 ps following 355 nm laser flash excitation of I in methanol.

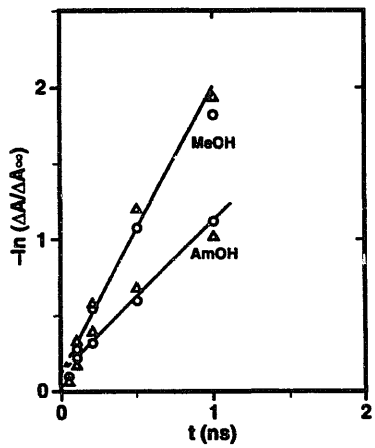

Fig. 5. First-order kinetic analyses of recovery of ground-state absorption (Δ) and decay of 450 nm transient absorption (O) following laser flash excitation of I in methanol (MeOH) and 1-pentanol (AmOH).

demonstrate a viscosity dependence. The non-zero intercepts of the kinetic plots suggest that there is also a much faster component to recovery of the ground state which accounts, however, for no more than ca 10% of total excitation energy dissipation. This result differs from that of Åberg et al. [8] who found ground-state recovery to be essentially complete within ca. 50 ps for 1,1′-diethyl 4,4′-cyanine in hexanol.

A reviewer has proposed that our time-resolved data can be accounted for by very fast (ps) ground-state recovery, with partitioning between isomerized and unisomerized I. Absorption recovery on the nanosecond time scale accordingly corresponds to reestablishment of equilibrium between the two possible ground-state isomers. There are two difficulties with this model. First of all, bleaching at 422 nm corresponds to disappearance of ground-state *syn*-I; its photoisomer, *anti*-I, absorbs at 392 nm, not 450 nm. Secondly, in other cyanine dyes studied [22,24], ground-state isomerization occurs on the microsecond or millisecond, not nanosecond, time scale.

We prefer to assign the long-lived state giving rise to the 450 nm absorption as the twisted state of I in which the dihedral angle between the planes of the two benzthiazole rings is ca. $\pi/2$. This configuration corresponds to the minimum on the potential surface corresponding to the lowest excited singlet state [8]. Accordingly, the excited-state potential energy minimum is reflected in the ground-state potential surface, leading to occurrence of a "conical intersection" of potential surfaces. Such conical intersections appear to provide a universal decay route for excited conjugated, polyatomic molecules [25], and are usually proposed for the radiationless deactivation of cyanine dyes [22,24a,26]. Most authors assume, however, that crossing from S_1 to S_0 potential surfaces at this point occurs rapidly, compared to the molecular relaxations leading to and from the funnel state. In our interpretation, however, the lifetimes measured by the plots of Fig. 5 correspond to the decay of this funnel state to the ground-state surface. The schematic of potential energy of ground and first excited states as a function of the torsional angle, based on Åberg et al.'s scheme

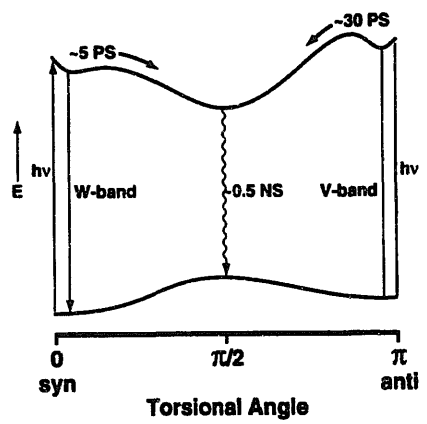

Fig. 6. Proposed potential energy surface for syn–anti photoisomerization of I; time constants correspond to experimentally determined values in methanol at ambient temperature.

[8], is shown in Fig. 6. Unlike for certain carbocyanine dyes [24b,27], all the experimental results can be rationalized without invoking intersystem crossing coupled to the torsional relaxation which may be a unique feature of dyes with longer polymethine chains.

3.4. Fluorescence quenching and enhancement

If the V- and W-band emissions arise from rapidly equilibrating syn- and anti-isomers, of I, static quenching should affect only the overall intensity of fluorescence, and not the relative intensities of V- and W-emissions. On the other hand, significant dynamic quenching of the emissive states of V- and W-I is not feasible, even under conditions of diffusion-limited kinetics, owing to the short radiative lifetimes of both species.

Quenching with *N,N*-dimethylaniline (DMA), *N,N*-dimethyl-p-toluidine (DMT) and tri-n-propyl amine (TPA) was studied in methanol. All three compounds should be thermodynamically capable of electron-transfer quenching [28]. Ionization potential (IP) values are −7.35 eV for DMA, −7.12 eV for DMT, and −7.25 eV for TPA [29]. We estimated the IP of I to be ca. −7.6 eV from its solution phase oxidation potential at a Pt electrode [30], using Miller's equation [31]. With DMA, quenching of the V-band followed the Stern–Volmer form, with $K=1.48\ M^{-1}$, intercept = 1.00, and $r=0.994$. Quenching of V-band emission by DMT also exhibited a Stern–Volmer quencher concentration dependence, with $K=2.75\ M^{-1}$, intercept = 1.04, and $r=0.989$. Data are given in Table 3. Surprisingly TPA did not quench fluorescence of I.

The slopes of these correlations are at least an order of magnitude too large for diffusion-limited dynamic quenching. We thus infer formation of ground-state complexes between I and DMA or DMT. These complexes must have similar absorption spectra to free I, insofar as no changes in the absorption spectrum of I were detected on addition of 0.35 M of either quencher. In this case K can be identified with the association constant for the complex. Since TPA did not form such a complex, we conclude that I may be inclined to form π- but not σ-complexes, and that static quenching ability is governed by steric rather than thermodynamic issues. To our knowledge, π-complexation of cyanine dyes in the ground state has not been previously reported.

If the W- and V-isomers of I are, in fact, rapidly equilibrating, the ratio of their concentrations is solution should not be altered by complexation of either form. With DMA, quenching of W-band fluorescence was observed, and the concentration dependence followed the Stern–volmer form with $K=1.46\ M^{-1}$, intercept = 1.00, and $r=0.996$. These parameters are in good agreement with those for V-band quenching, consistent with the assumption of rapid equilibration of the isomers. With DMT, however, enhancement of the W-band emission was observed.

We hypothesized in this case that the complexed W-isomer of I is more efficiently fluorescent than the free dye. Accordingly the observed fluorescence intensity, I, comprises contributions from the free dye, $I_o\ (1-f_{complex})$, and complexed dye, $I_{complex}$. Thus, given

$$f_{complex}=K[DMT]/(1+K[DMT]) \quad (5)$$

$$I_{complex}=I-I_o/(1+K[DMT]) \quad (6)$$

the contribution of the complexes species to the observed fluorescence intensity can be estimated. It follows that the normalized complex emission intensity,

$$I_{complex}/(I_o f_{complex})=\Phi_f(\text{complex})/\Phi_f(\text{free dye}) \quad (7)$$

should be independent of [DMT].

Values of observed I, $I_{complex}/I_o$ from Eq. (6), and $I_{complex}/(I_o f_{complex})$ for W-band emission of I in presence of DMT are given in Table 4, using $K=2.75\ M^{-1}$ from V-band quenching. It is obvious that $I_{complex}/(I_o f_{complex})$ actually decreases with increasing [DMT], i.e. fluorescence from complexed I is also quenched by DMT. A Stern–Volmer plot for this quenching is shown in Fig. 7; slope is $2.47\ M^{-1}$, $r=0.983$, and intercept = 0.20. The physical significance of this intercept is the reciprocal of the ratio of fluorescence quantum efficiencies for complexed and free dye according to Eq. (7); we estimate $\Phi_f(\text{complex})=(0.015\pm0.004)$. Observation of fluorescence enhancement only for the W-band of I suggests that only the syn-isomer of the dye may participate in complex formation.

With DMA, on the other hand, either $\Phi_f(\text{complex}) \leq 5\times10^{-4}$ (instrumental limit of detection), or else this quencher does not form a complex with the W-isomer of I. In either case the difference in behavior of the two subtly different complexing reagents is remarkable and worthy of

Table 3
Quenching of V-band fluorescence from I in methanol by DMA and DMT

[Q]	I_o/I (DMA)	I_o/I (DMT)
0.05 M	1.06	1.17
0.10	1.145	1.38
0.15	1.22	1.48
0.20	1.29	1.61
0.25	1.37	1.76
0.35	1.52	1.97

Table 4
Effect of DMT on W-band fluorescence from I in methanol

[Q]	I (DMT)	$I_{complex}/I_o$	$I_{complex}/(I_o f_{complex})$
0 M	176 (a.u.)	0	–
0.05	210	0.31	2.63
0.10	220	0.47	2.17
0.15	233	0.61	2.03
0.20	206	0.52	1.49
0.25	190	0.48	1.17
0.35	170	0.45	0.91

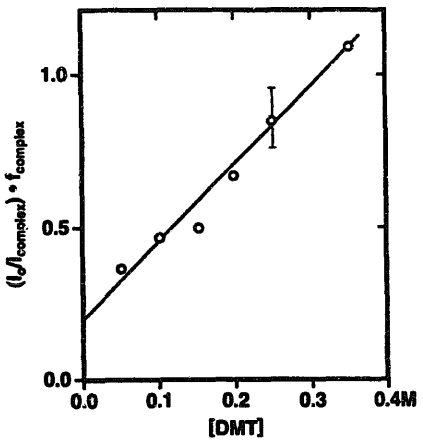

Fig. 7. Stern–Volmer plot for quenching of fluorescence attributed to π-complexed I in methanol: $(I_o/I_{complex}) \cdot f_{complex}$ vs. [DMT]. Error bar is representative. Intercept corresponds to $[\Phi_f(\text{complex})/\Phi_f(\text{free dye})]^{-1}$.

further investigation. One possibility is that the radiative lifetimes of both the DMA and DMT complexes of I are limited by the rate of intra-complex electron transfer quenching. Slower electron transfer from DMA to excited I than from DMT may be rationalized if both processes are understood as occurring in the Marcus inverted regime, consistent with the electrochemical data.

3.5. Adsorption of I to AgBr

A 2.5×10^{-6} M solution of dye I was added to a 1×10^{-4} M AgBr nanosol in absolute ethanol. Its absorption spectrum is shown in Fig. 8. Subtraction of the spectrum of Fig. 1 indicated a small contribution ($D_{max}\leq0.025$) of red-shifted absorption centered on 445 nm. The fluorescence spectrum obtained from this mixture with $\lambda_{ex}=420$ nm is shown in Fig. 9. It appears similar to the spectrum of Fig. 2(a) with further attenuated V-band emission and enhanced W-band emission. When the excitation spectrum was recorded with $\lambda_{em}=500$ nm, a bimodal distribution of activity was observed, also shown in Fig. 8, corresponding to a combination of the W-band action spectrum and a new band centered on 454 nm ($\Delta\nu_{1/2}=15\,000\,cm^{-1}$). This new band was approximately congruent with the red-shifted contribution to absorption. Such red shifts are characteristic on adsorption of cyanine dyes to AgBr, and are usually attributed to the high dielectric constant of the solid substrate [32]. These observations imply that I is adsorbed onto AgBr as the W-isomer, and that the Stokes shift associated with W-isomer emission is significantly reduced thereby, consistent with restricted conformational relaxation in the adsorbed state [6,33]. Insofar as we expect that I should adsorb to AgBr preferentially in the syn-conformation [1a,32], this interpretation further confirms the identity of the W-species with *syn*-I.

Excitation directly into this new band at $\lambda_{ex}=450$ nm yielded only the fluorescence distribution centered on 484 nm, as obtained by deconvolution of the emission spectrum obtained with 420 nm excitation (Fig. 9). Again, by comparison of integrated fluorescence intensity to that of the standard, Coumarin 343, we estimate $\Phi_f=(0.12\pm0.02)$. We assign this red-shifted absorption and emission to dye adsorbed on AgBr. We estimate from the difference spectrum of Fig. 8 that ca. 10% of the dye, $(2.5\pm0.5)\times10^{-7}$ M, is adsorbed to AgBr under these conditions. Assuming a projection area, $a_o=100$ Å^2, for one molecule of I adsorbed flat onto the surface, and an individual particle surface of 1.1×10^4 Å^2, we estimate that monolayer coverage corresponds to 1.1×10^{-6} M dye adsorbed. Under our conditions we thus obtain approximately 0.2 monolayer coverage. This level is too low for photophysics of adsorbed I to be complicated by dimer formation [6].

Enhanced fluorescence efficiency in the red-shifted band relative to that of free dye in solution is consistent with this assignment [6]. It is usually assumed that adsorption quenches the radiationless deactivation modes associated with torsional relaxation. The principal non-radiative pathway for dye deactivation then involves electron (or energy) transfer to the AgBr substrate. This is the process responsible for photographic sensitivity [1,32–35]; it occurs with rate constant k_s. Then, ignoring other radiationless deactivation channels which are likely to be of minor significance for adsorbed I,

$$\Phi_f=\tau_{nat}^{-1}/(k_s+\tau_{nat}^{-1}) \quad (8)$$

and using the solution value of $\tau_{nat}=2$ ns in Eq. (7), we estimate $k_s=(3.6\pm0.6)\times10^9$ s^{-1}. This value is in good agreement with the estimates of Muenter [34] and of Tani et al. [35] for the rate constant for electron transfer from other

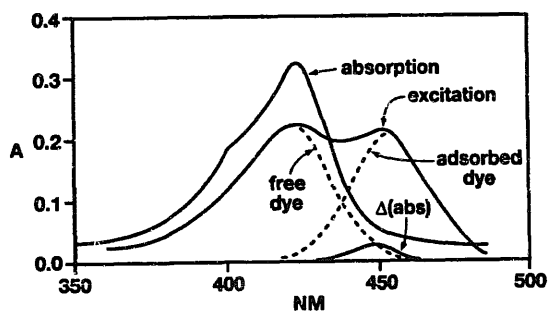

Fig. 8. Absorption and excitation ($\lambda_{em}=500$ nm) spectra of 2.5×10^{-6} M I in the presence of 1.0×10^{-4} M AgBr nanosol, showing differential absorption (430–460 nm) and deconvolution of the excitation spectrum (dashed lines).

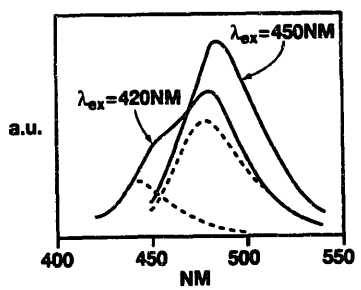

Fig. 9. Fluorescence spectra of 2.5×10^{-6} M I in the presence of 1.0×10^{-4} M AgBr nanosol, with $\lambda_{ex}=420$ nm, showing deconvolution, and $\lambda_{ex}=450$ nm.

photoexcited cyanine dyes to the conduction band of AgBr. From the model of Tani et al., based on the Marcus treatment of electron transfer, we infer that ΔG for electron injection is ca. −0.18 eV. Using a value of −1.34 V for the conduction band of AgBr [35], we find that this estimate corresponds to $E_{red} = -1.52$ V (vs. SCE) for **I**, which is in exact agreement with electrochemical measurement [30].

Both DMA and DMT quenched the fluorescence from adsorbed **I**. The quenching failed to follow the Stern–Volmer form, but rather data obtained with both amines followed the form

$$\ln(I_0/I) = \alpha[Q] \quad (9)$$

where [Q] designates the solution concentration of a generic quencher. Plots of this relationship for both quenchers are shown in Fig. 10; in both cases points fall on the same line with slope 4.66 M^{-1} and $r = 0.9945$. This analytical form corresponds to that derived by Perrin [36] and originally applied to static energy transfer quenching, e.g. long-range energy or electron transfer, in solid solution [36b]. In the present case, energy transfer quenching is infeasible. Accordingly we assign quenching to long-range electron transfer between adsorbed quencher and excited adsorbed **I**.

Alternative quenching models in which:
(a) adsorbed quencher displaces **I** from the AgBr surface; or
(b) quencher molecules in solution interact dynamically with adsorbed **I**;
were considered but discarded, as both would relate observed fluorescence intensity to [Q] according to an expression of the Stern–Volmer form.

By operation of the long-range static electron transfer mechanism of quenching the principal consequence of photoexcitation of **I** will be formation of the corresponding radical therefrom by one-electron reduction. This species will be a stronger reducing agent than photoexcited dye itself. Intermediacy of such species in spectra sensitization of silver halide photography has been proposed [37]. Electron transfer quenching of photoexcited dye to generate such radical species has been the accepted interpretation for a number of years of the phenomenon of supersensitization observed in photographic media [37,38]. The present results can be taken as further experimental confirmation for the feasibility of this pathway.

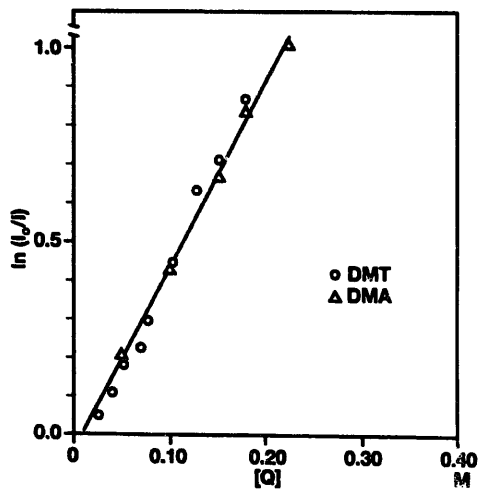

Fig. 10. Quenching of fluorescence of AgBr-adsorbed **I** by DMA and DMT, analyzed according to Eq. (9).

Acknowledgements

We thank Dr. M.C. Palazzotto of the 3M Corporate Research laboratories for gift of the quenchers. Expert reconfiguration of the fluorimeter to enable this study was carried out by Ms Susan Hill. Helpful discussion with Prof. R.W. Yip, Université de Québec á Montréal is also acknowledged with appreciation. Time-resolved spectroscopy was carried out at the Canadian Centre for Fast Laser Spectroscopy, Concordia University, Montréal. The hospitality and helpful counsel of Prof. N. Serpone in Montréal is acknowledged with gratitude as is the expert technical assistance of Mr. Reza Danesh with the experiments there. GAUSSIAN 94 computations were carried out on the Cray C90 of the Minnesota Supercomputer Institute. Dr. M.K.L. Bicking, ACCTA, Inc., provided helpful comments during the preparation of the manuscript.

References

[1] (a) G.R. Bird, *ACS Symp. Ser., 200* (1982) 1; (b) D.M. Sturmer and A.P. Marchetti, in J. Sturge, A. Shepp and V. Walworth (eds.), *Imaging Materials and Processes*, Van Nostrand-Reinhold, New York, 1989, pp. 96; (c) M.T. Spitler, *J. Imaging Sci., 35* (1991) 351; (d) S. Dähne, *J. Imaging Sci., 38* (1994) 101.
[2] M. Krieg, M.B. Srichai and R.W. Redmond, *Biochim. Biophys. Acta, 1151* (1993) 168, and references cited therein.
[3] (a) A.N. Tarnovskii, T.K. Razumova, E.P. Shchelkina and T.V. Veselova, *Opt. Spectrosc., 74* (1993) 65; (b) M. Kaschke, N.P. Ernsting, B. Valeur and J. Bourson, *J. Phys. Chem., 94* (1990) 575; (c) M. Maeda, *Laser Dyes: Properties of Organic Compounds for Dye Lasers*, Academic Press, New York, 1984.
[4] (a) R. Humphry-Baker, M. Gratzel and R. Steiger, *J. Amer. Chem. Soc., 102* (1980) 847; (b) T. Kunitake, *J. Amer. Chem. Soc., 104* (1982) 4261.
[5] A.P. Ischchenko, *Usp. Khim., 60* (1991) 1708.
[6] D. Fassler and M. Baezold, *J. Photochem. Photobiol., A: Chem., 64* (1992) 359.
[7] M. Watanabe, W. Herren and M. Morita, *J. Luminesc., 58* (1994) 198.
[8] U. Åberg, E. Åkesson, J.-L. Alvarez, I. Fedchenia and V. Sundstrom, *Chem. Phys., 183* (1994) 269.
[9] (a) C. Rulliére, *Chem. Phys. Lett., 43* (1976) 303; (b) U. Petrov and C. Rempel, *Chem. Phys. Lett., 148* (1988) 26.
[10] V. A. Tkachev, E. I. Maltsev and A.V. Vannikov, *Khim. Fiz., 8* (1989) 42.
[11] M.R.V. Sahyun, D.K. Sharma and N. Serpone, *J. Imaging Sci., 39* (1995) 377.
[12] (a) K.L. Sala, R.W. Yip and R. LeSage, *Appl. Spectrosc., 37* 91983) 273; (b) W. Yu, in C.V. Shank, E.P. Ippen and S.L. Shapiro (eds.), *Picosecond Phenomena*, Springer, Berlin, 1978, pp. 346ff.
[13] N. Serpone, D.K. Sharma, J. Moser and M. Graetzel, *Chem. Phys. Lett., 136* (1987) 47, and references cited therein.
[14] J.J.P. Stewart, *J. Computational Chem., 10* (1989) 209.

[15] W.J. Hehre, SPARTAN, version 4.0, © 1995, Wavefunction, Inc.
[16] M.J. Frisch, G.W. Trucks, M. Head-Fordon, P.M.W. Gill, M.W. Wong, J.B. Foresman, B.G. Johnson, H.B. Schlegel, M.A. Robb, E.S. Replogle, R. Gomperts, J.L. Andres, K. Raghavachari, J.S. Binkley, C. Gonzalez, R.L. Martin, D.L. Fox, D.J. DeFrees, J. Baker, J.J.P. Stewart and J.A. Pople, GAUSSIAN 94, © 1994, Gaussian, Inc.
[17] J.S. Binkley, J.A. Pople and W.J. Hehre, *J. Amer. Chem. Soc., 102* (1980) 939.
[18] S.J. Strickler and R.A. Berg, *J. Chem. Phys., 37* (1962) 814.
[19] D. Noukakis, M. van der Auweraer, S. Toppet and F.C. DeSchryver, *J. Phys. Chem., 99* (1995) 11860.
[20] M. Vogel and W. Rettig, *Ber. Bunsenges. Phys. Chem., 91* (1980) 1241.
[21] S. Murphy, B. Sauerwein, H.G. Drickamer and G.B. Schuster, *J. Phys. Chem., 98* (1994) 13476.
[22] P.F. Aramendía, R. Martin Negri and E. San Román, *J. Phys. Chem., 98* (1994) 3165.
[23] E.M. Kosower and D. Huppert, *Ann. Rev. Phys. Chem., 37* (1986) 127, and references cited therein.
[24] (a) E. Vauthey, *Chem. Phys., 196* (1995) 569, and references cited therein; (b) G. Ponterini and M. Caselli, *Ber. Bunsenges Phys. Chem., 96* (1992) 564.
[25] P. Celani, M. Garavelli, S. Ottani, F. Bernardi, M.A. Robb and M. Olivucci, *J. Amer. Chem. Soc., 117* (1995) 11584, and references cited therein.
[26] A.K. Chibisov, G.V. Zakharova, H. Görner, Yu. A. Sogulyaev, I.L. Mushkalo and A.I. Tolmachev, *J. Phys. Chem., 99* (1995) 886.
[27] N. Serpone and M.R.V. Sahyun, *J. Phys. Chem., 98* (1994) 734.
[28] D. Rehm and A. Weller, *Isr. J. Chem., 8* (1970) 259.
[29] J.L. Franklin and P. Haug, in *Handbook of Chemistry and Physics*, 53rd edn., Chemical Rubber Co., Cleveland, OH, 1972, pp. E-62ff, and references cited therein.
[30] J. Stanienda, *Naturwiss., 47* (1960) 353, 512; trivially different values have been reported for this dye more recently by J.R. Lenhard, *J. Imaging Sci., 30* (1986) 27.
[31] L.L. Miller, G.D. Nordblom and E.A. Mayeda, *J. Org. Chem., 37* (1972) 916.
[32] W. West and B.H. Carroll, in T.H. James (ed.), *Theory of the Photographic Process*, 3rd edn., Macmillan, New York, 1966, pp. 246ff.
[33] D. Fassler, M. Baezold and D. Baezold, *J. Mol. Struct., 174* (1988) 383.
[34] A.A. Muenter, *J. Phys. Chem., 80* (1976) 2178.
[35] T. Tani, T. Suzumoto, K. Kemnitz and K. Yoshihara, *J. Phys. Chem., 96* (1992) 2778; T. Tani, T. Suzumoto and K. Ohzeki, *J. Phys. Chem., 94* (1990) 1298.
[36] (a) J. Perrin, *C.R. Acad. Sci. (Paris) 178* (1924); *184* (1927) 1097; (b) V.L. Ermolaev, *Sov. Fiz. Dokl., 6* (1962) 600.
[37] (a) D. Fassler, K.-H. Feller, R. Gadonas, V. Krasauskas, A. Pelakauskas and A. Piskarkas, *J. Inf. Rec. Mater., 17* (1989) 267; (b) J. Siegel, D. Fassler, M. Friedrich, J.V. Grossmann, U. Kempka and H. Pietsch, *J. Photogr. Sci., 35* (1987) 73; (c) J.W. Mitchell, *J. Imaging Sci., 30* (1986) 91.
[38] (a) P.B. Gilman, Jr., *Photogr. Sci. Eng., 18* (1974) 418, and references cited therein; (b) T. Tani, Y. Sano and M. Saito, *Photogr. Sci. Eng., 23* (1979) 240.